The Journal of Infectious Diseases

BRIEF REPORT

Tissue Pharmacologic and Virologic Determinants of Duodenal and Rectal Gastrointestinal-Associated Lymphoid Tissue Immune Reconstitution in HIV-Infected Patients Initiating Antiretroviral Therapy

David M. Asmuth,[1] Corbin G. Thompson,[2] Tae-Wook Chun,[3] Zhong-Min Ma,[4] Surinder Mann,[1] Talia Sainz,[5] Sergio Serrano-Villar,[6] Netanya S. Utay,[7] Juan Carlos Garcia,[1] Paolo Troia-Cancio,[1] Richard B. Pollard,[1] Christopher J. Miller,[1,4] Alan Landay,[8] and Angela D. Kashuba[2]

[1]University of California, Davis Medical Center, Sacramento, [2]Eshelman School of Pharmacy, University of North Carolina, Chapel Hill, [3]Laboratory of Immunoregulation, National Institute of Allergy and Infectious Diseases, National Institutes of Health, Bethesda, Maryland, and [4]California National Primate Research Center, Davis; [5]University Hospital La Paz and IdiPAZ, and [6]University Hospital Ramón y Cajal and IRYCIS, Madrid, Spain; [7]University of Texas Medical Branch, Galveston, and [8]Rush University Medical Center, Chicago, Illinois

Plasma, duodenal, and rectal tissue antiretroviral therapy (ART) drug concentrations, human immunodeficiency virus (HIV) RNA and HIV DNA copy numbers, and recovery of mucosal immunity were measured before and 9 months after initiation of 3 different ART regimens in 26 subjects. Plasma and tissue HIV RNA correlated at baseline and when 9-month declines were compared, suggesting that these compartments are tightly associated. Antiretroviral tissue:blood penetration ratios were above the 50% inhibitory concentration values in almost 100% of cases. There were no correlations between drug concentrations and HIV DNA/RNA. Importantly, no evidence was found for residual viral replication or deficient tissue drug penetration to account for delayed gastrointestinal-associated lymphoid tissue immune recovery.

Keywords. gastrointestinal-associated lymphoid tissue; immune reconstitution; HIV persistence; antiretroviral concentration; ART tissue penetration.

The profound loss of mucosal CD4$^+$ T-cells that occurs during acute human immunodeficiency virus (HIV) infection is usually not restored by subsequent control of viremia and increased systemic CD4$^+$ T-cell counts [1]. Indeed, as with systemic CD4$^+$ T-cell recovery, there is wide variation in patients' mucosal CD4$^+$ T-cell recovery (known as immune reconstitution) following combination antiretroviral therapy (cART) initiation that is independent of peripheral blood CD4$^+$ T-cell recovery [2].

There are several hypotheses to account for the discordant recovery of immune cell populations between compartments in the gut and peripheral blood with the early focus being on persistent HIV cytopathic effect [1]. While low-level residual viral replication detected throughout the gastrointestinal tract has been reported, the ratio of unspliced RNA to DNA is similarly low across tissue and vascular compartments, as would be expected if they were in equilibrium [3]. Currently, limited longitudinal data examining gastrointestinal-associated lymphoid tissue (GALT) antiretroviral penetration coupled with virologic kinetics have been published [4, 5]. We performed a 3-arm, randomized clinical trial of different cART regimens to explore primarily which regimen(s) promoted mucosal immune reconstitution [6]. This report focuses on the virologic and pharmacologic analysis to explore the distribution of HIV RNA and HIV DNA and the pharmacokinetics of cART into tissue compartments. We hypothesized that if residual viremia drives blunted immune reconstitution in GALT, then a correlation between reduced drug tissue penetration and the size of viral reservoirs should be evident.

METHODS

Study Design

This pilot, randomized clinical trial enrolled chronically HIV-infected patients naive to antiretroviral therapy (ART) with CCR5 tropism by TrofileES (Monogram Biosciences, South San Francisco, California) and sensitivity to all selected ART agents by reverse-transcription polymerase chain reaction (PCR) sequencing. Subjects were randomized to 1 of 3 cART regimens: either maraviroc (MVC), MVC + raltegravir (RAL), or efavirenz (in-class switch was permitted in the case of side effects), each in combination with tenofovir disoproxil fumarate/emtricitabine (TDF/FTC) administered at standard doses after completing baseline endoscopy as previously published [6]. Phlebotomy and upper and lower endoscopy were performed prior to initiating ART and after 9 months of therapy. In addition, 12 HIV-negative controls who were similar to the HIV-infected cohort underwent a single set of identical procedures.

Ethics Statement

All participants provided signed informed consent as approved by the University of California, Davis Institutional Review Board (ClinicalTrials.gov: NCT00870363).

Sample Preparation

Intestinal biopsies were placed immediately in either liquid nitrogen, paraformaldehyde, or sterile media. Peripheral blood mononuclear cells (PBMCs) were isolated using Ficoll-Hypaque (Pfizer-Pharmacia, New York, New York). Single-cell

Received 6 February 2017; editorial decision 10 August 2017; accepted 15 August 2017; published online August 23, 2017.

Presented in part: 22nd Conference on Retroviruses and Opportunistic Infections, Seattle, Washington, 23–26 February 2015 [abstract 548]; and Eighth International AIDS Society (IAS) Conference on HIV Pathogenesis, Treatment and Prevention, Vancouver, British Columbia, Canada, 19–22 July 2015 [abstract MOPEA006].

Correspondence: D. M. Asmuth, MD, Professor of Medicine, Division of Infectious & Immunologic Diseases, 4150 V Street, PSSB G500, UC Davis, Medical Center, Sacramento, CA 95817 (dasmuth@ucdavis.edu).

The Journal of Infectious Diseases® 2017;216:813–8

DOI: 10.1093/infdis/jix418

suspensions were generated by collagenase digestion (a single lot from Sigma-Aldrich, St Louis, Missouri) for 3 cycles of 15 minutes followed by sterile saline washes. PBMCs and tissue single-cell suspension were stained with a panel of fluorochrome antibodies (see Supplementary Methods) and interrogated on a customized Beckman-Dickenson LSR-II [6].

Immunofluorescent antibody analysis was performed using polyclonal anti-CD3 rabbit serum (Dako, Carpinteria, California) and monoclonal anti-CD4 or anti-CD8 mouse serum (Leica, Buffalo Grove, Illinois) for the primary antibodies. Binding of CD3 and CD4, as well as CD3 and CD8 receptors, was detected using AlexaFluor 488–labeled polyclonal goat antirabbit immunoglobulin G (IgG) (Molecular Probes, Eugene, Oregon) and AlexaFluor 568–labeled polyclonal goat antimouse IgG (Molecular Probes). Positive cells were counted by a single observer (Z.-M. M.) and presented as cells per square millimeter of intestinal lamina propria [2].

Measurement of HIV RNA and DNA

DNA was digested from cell pellets (1×10^6 PBMCs or intestinal single cell suspension) with XbaI, and 500 ng of DNA was subjected to PCR (Bio-Rad Laboratories) according to the manufacturer's specifications. The amplification reaction was carried out using HIV-specific primers and probes as described in the Supplementary Materials. Serially diluted ACH-2 DNA (from 40 000, 8000, 1600, 320, 64, 12.8, 2.56, and 0.56 cell equivalents per well in triplicates) was also subjected to the PCR conditions above to obtain standard curves. The level of detection is 2.56 copies/cell [7].

For detection of the unspliced form of HIV type 1 (HIV-1) RNA, total RNA was isolated from plasma and whole snap-frozen tissue by using RNeasy Mini Kit (Qiagen), according to the manufacturer's specifications (see Supplementary Materials for synthesis of cDNA and primers that were used) [7]. HIV copy numbers were determined per microgram of RNA from tissue samples with a limit of detection of 2.56 copies/μg and normalized by duodenal $CD4^+$ T-cell numbers determined by immunofluorescent antibody.

Measurement of Plasma and Tissue Drug Concentrations

Drug concentrations were quantified by liquid chromatography–tandem mass spectrometry analysis using methods similar to those previously published [8–10]. See Supplementary Methods for additional details.

Tissue penetration ratios (TPRs) were calculated by dividing the tissue by the plasma concentration after the tissue concentrations were converted to nanograms per milliliter (to convert volume to mass, tissue density was assumed to be 1.06 g/mL). Tenofovir (TFV) and FTC TPRs were not significantly different across dosing cohorts in either GALT site ($P > .05$); therefore, these 2 drugs were pooled for further comparisons. Additionally, MVC TPRs between the MVC and MVC + RAL cohort were not significantly different and these values were also pooled.

To determine whether tissue antiretroviral (ARV) concentrations were above the reported 50% or 90% inhibitory concentration values (IC_{50} and IC_{90}, respectively) obtained from in vitro studies, the measured ART concentrations in tissue (nanograms per milligram) were divided by the listed IC_{50} (or IC_{90} where reported) values reported in the package insert from each ART. When IC_{50} ranges were reported, the maximum IC_{50} for wild-type HIV-1 clinical isolates was used to provide the most conservative estimate.

Statistical Methods

Nonparametric methods were used throughout as described in the Supplementary Methods. Results are expressed as median with interquartile range (IQR).

RESULTS

Twenty-six HIV-infected patients naive to cART were evaluable for baseline and 9-month analysis following randomization. The baseline characteristics are shown in Table 1. GALT immune reconstitution was blunted in both tissue compartments especially when viewed in the context of immune reconstitution that occurs in the peripheral blood following cART. Baseline median $CD4^+$ T-cell density in the lamina propria was 48.1 (IQR, 30.6–184.4) and 45.2 (IQR, 28.8–73.4) cells/mm^2 in the duodenum and rectum, respectively, increasing to 150 (IQR, 96.9–251.9) and 151.4 (IQR, 80.9–199.6) cells/mm^2 after 9 months of cART in the duodenum and rectum, respectively. These values compare to 565.9 (IQR, 444.8–676.9) and 395 (IQR, 331.6–493.7) $CD4^+$ cells/mm^2 in the duodenum and rectum of control subjects, respectively. In addition, peripheral blood absolute $CD4^+$ T-cell counts increased to 523 (IQR, 364–702) cells/dL after 9 months, which was in the normal range (>450 cells/dL) for 75% of subjects.

Clinically, all individuals rapidly achieved and maintained HIV suppression (plasma viral load [pVL] ≤20 copies/mL). Median tissue HIV RNA declined from 12 852 (IQR, 2134–64 476) to 2.5 copies/$CD4^+$ T cell (IQR, 2.5–3.1) in the rectum ($P < .001$) and from 74 (IQR, 8.3–1482) to 2.5 copies/$CD4^+$ T-cell (IQR, both <2.5) in the duodenum ($P < .001$), extracted from whole tissue. Undetectable tissue HIV RNA was measured from tissue after 9 months of cART in 17 of 26 and 15 of 25 subjects in the duodenal and rectal tissue samples, respectively. Cell-associated DNA copies/10^6 cells declined from a median of 2255 (IQR, 1188–4317) to 1418 (IQR, 728–2648) in the peripheral blood ($P = .003$), from 261 (IQR, 154–650) to 30 (IQR, 13–49) in the rectal cells ($P = .03$), and from 101 (IQR, 4–355) to 6 (IQR, 2.5–69) in the duodenal cells ($P < .001$). Interestingly, pVL correlated with tissue HIV RNA at baseline and when correlating the magnitude of changes from baseline to month 9, suggesting that these compartments are tightly associated and potentially in equilibrium (Spearman $r = 0.54$, $P = .005$ and $r = 0.55$, $P < .003$ for duodenal tissue RNA at baseline and 9-month changes, respectively; Spearman $r = 0.44$, $P = .02$ and $r = 0.44$, $P < .03$ for rectal tissue RNA at baseline and 9-month changes, respectively).

Table 1. Baseline Demographics of Study Participants

Characteristic	Normal Controls	HIV Infected
No. of subjects	12	26
Age, y, median (IQR)	35 (29–42)	37 (25–42)
Male sex, No. (%)	7 (58)	22 (85)
Race, No. (%)		
Asian	1 (8.3)	2 (7.7)
Black	1 (8.3)	10 (38.4)
White	9 (55.0)	12 (46.1)
Pacific Islander	1 (8.3)	1 (3.8)
Hispanic	0 (0)	1 (3.8)
$CD4^+$ T-cell count, cells/mm^3, median (IQR)	NA	436 (283–572)
CD4/CD8 ratio, median (IQR)	1.6 (1.2–2.6)	0.43 (0.33–0.60)
HIV RNA level, copies/mL, median (IQR)	NA	14 130 (4059–34 009)

				P Value		
		Month 0	Month 9	HIV^- vs HIV^+ Month 0	HIV^- vs HIV^+ Month 9	Delta Change in HIV^+
Blood $CD4^+$ T-cells/mm^3, median (IQR)	…	436 (283–572)	693 (452–848)	…	…	<.001
Rectal $CD4^+$ T-cells/mm^2, median (IQR)	395 (340–478)	51 (29–88)	135 (54–167)	<.001	<.001	.013
Duodenal $CD4^+$ T-cells/mm^2, median (IQR)	566 (509–688)	48 (31–184)	158 (116–254)	<.001	<.001	.011

Abbreviations: HIV, human immunodeficiency virus; IQR, interquartile range; NA, not available.

Table 2. Plasma and Tissue Antiretroviral Therapy Concentrations by Liquid Chromatography–Mass Spectrometry

	NNRTI (n = 8)		MVC (n = 10)		MVC + RAL (n = 8)		
	Plasma, ng/mL		Plasma, ng/mL		Plasma, ng/mL		*P* Value
	FTC	419.2 (281.4–629.5)	FTC	126.1 (59.9–357.4)	FTC	326.5 (181.5–460.9)	.198
	TFV	126.5 (79.9–147.4)	TFV	55.9 (22.4–63.2)	TFV	64.1 (54.7–73.5)	.007
	EFV (n = 6)	2459.0 (1485.7–5238.2)	MVC	94.5 (60.5–126.5)	MVC	71.3 (39.6–80.2)	
	NVP (n = 2)	7117.3 (5516.3–8718.3)			RAL	397.0 (93.4–1131.3)	
	Tissue, ng/mg		Tissue, ng/mg		Tissue, ng/mg		
Rectal EFV (n = 6)		8.6 (6.4–11.9)	Rectal MVC	5.3 (2.2–11.5)	Rectal MVC	2.9 (1.9–5.4)	
Duodenal EFV (n = 6)		10.7 (8.4–15.0)	Duodenal MVC	0.7 (0.3–1.4)	Duodenal MVC	0.6 (0.4–0.9)	
Rectal NVP (n = 2)		11.1 (8.7–13.6)			Rectal RAL	0.4 (0.3–1.0)	
Duodenal NVP (n = 2)		11.1 (10.8–11.4)			Duodenal RAL	0.1 (0.07–0.3)	
Rectal	FTC	1.0 (0.4–2.2)	FTC	1.4 (0.5–4.6)	FTC	0.8 (0.3–3.0)	.577
	FTC-tp*	688.4 (97.4–779.1)	FTC-tp*	244.4 (124.2–436.7)	FTC-tp*	292.3 (162.8–685.4)	.45
	TFV	1.4 (0.7–4.6)	TFV	3.9 (1.5–6.7)	TFV	1.7 (0.4–4.9)	.313
	TFV-dp*	1801 (1278–4056)	TFV-dp*	1941.6 (900.0–2540.5)	TFV-dp*	1057.1 (480.7–2785.5)	.934
Duodenal	FTC	1.6 (0.7–2.1)	FTC	0.8 (0.5–2.3)	FTC	1.2 (0.4–1.9)	.664
	FTC-tp*	636.6 (506.8–821.2)	FTC-tp*	234.2 (76.9–553.1)	FTC-tp*	233.0 (57.7–1000.6)	.649
	TFV	51.8 (24.8–99.9)	TFV	46.1 (8.6–109.0)	TFV	37.2 (6.9–86.5)	.823
	TFV-dp*	98 397 (85 793–153 445)	TFV-dp*	30 534 (6402–146 355)	TFV-dp*	44 476 (16 858–75 126)	.328

Data are presented as median and range. Subjects naive to antiretroviral therapy were randomized to receive either an NNRTI, MVC, or MVC + RAL, all in combination with tenofovir disoproxil fumarate/FTC. All other antiretroviral tissue concentrations were measured directly from biopsy tissue immediately snap-frozen during endoscopy. All samples were collected as trough levels after subjects had fasted in preparation for endoscopy after 9 months of treatment. Please note that the plasma concentrations are expressed as nanograms per milliliter, and tissue concentrations are expressed as nanogram per milligram; see the Methods on conversion from ng/mg to ng/mL, which was performed for the purposes of direct comparisons as illustrated in Figure 1.

Abbreviations: dp, diphosphate; EFV, efavirenz; FTC, emtricitabine; MVC, maraviroc; NNRTI, nonnucleoside reverse transcriptase inhibitor; NVP, nevirapine; RAL, raltegravir; TFV, tenofovir; tp, triphosphate.

*Intracellular FTC-tp and TFV-dp, the active forms of each agent, were measured from collagenase-digested, single-cell suspension preparations from biopsy tissue and are expressed as fmol/10^6 cells. Unfortunately, samples from PBMCs were not available to perform intracellular nucleotide concentrations, but these tissue intracellular levels equal or exceed published PBMC concentrations for FTC-tp and TFV-dp.

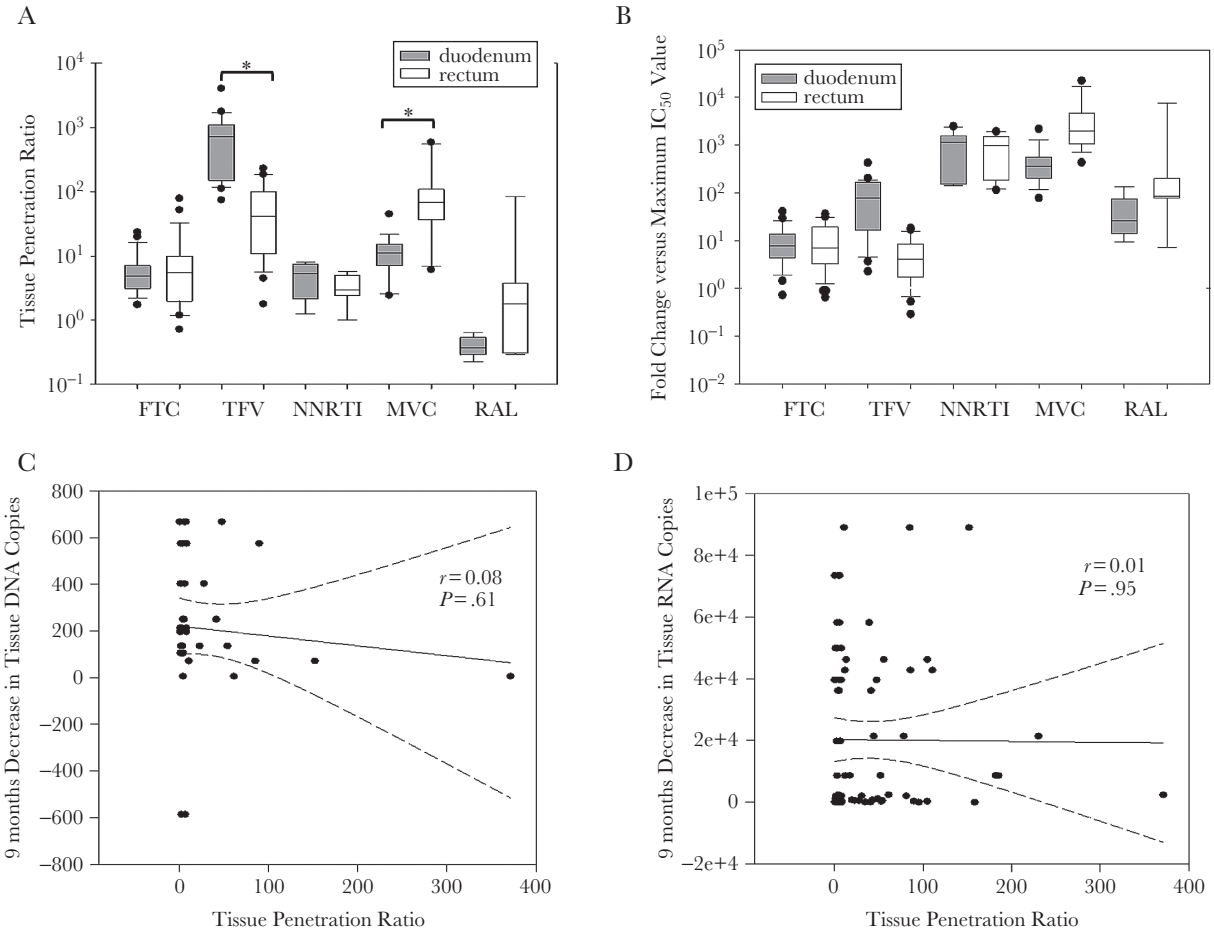

Figure 1. Antiretroviral tissue penetration ratios (TPRs) into small and large intestinal tissue. TPRs represent the extent of drug exposure in a given tissue relative to plasma and are calculated by dividing the tissue concentration (converted to ng/g) by a paired plasma concentration (ng/mL) using an assumed tissue density of 1.06 g/mL. *A*, Tenofovir (TFV) and emtricitabine TPRs were not significantly different across dosing cohorts in either the duodenum or rectum ($P > .05$); therefore, the TPRs for these 2 drugs were pooled when making further comparisons. Maraviroc (MVC) TPRs between the MVC and MVC + raltegravir (RAL) cohort were not significantly different and these values were also pooled. Significantly higher TFV penetration was observed in the duodenum compared to the colon, and MVC penetration was higher in the rectum vs the duodenum (*$P = .001$ for both). *B*, Tissue concentrations as reported in Table 2 were individually compared to the highest 50% inhibitory concentration (IC_{50}) reported in the literature (IC_{90} for efavirenz) after converting reported nM IC values to ng/mg. Tissue drug concentrations were above the IC_{50} nearly 100% of the time. These TPRs are consistent with what has been observed in previous studies of gut tissue, except for RAL, which was lower than what has been previously reported [11]. *C* and *D*, All drug penetration vs human immunodeficiency virus (HIV) decreases from baseline: No correlation was observed between tissue levels of viral decay assayed from biopsy specimens collected after 9 months of combination antiretroviral therapy. *C*, HIV DNA was measured in single-cell suspensions of rectal and duodenal tissue biopsies. *D*, HIV RNA was measured from rectal and duodenal tissue homogenates. Tissue penetration ratios are shown in (*A*). Abbreviations: FTC, emtricitabine; MVC, maraviroc; NNRTI, nonnucleoside reverse transcriptase inhibitor; RAL, raltegravir; TFV, tenofovir.

One hypothesis accounting for blunted intestinal immune reconstitution implicates reduced ARV penetration from plasma into gastrointestinal tissues [6]. There were no significant differences in plasma concentrations of any ARV between groups with the exception of plasma TFV, which was significantly higher in the nonnucleoside reverse transcriptase inhibitor cohort than in the MVC and MVC + RAL cohorts (Table 2). When comparing duodenal to rectal ARV concentrations, tenofovir diphosphate (TFV-dp), the intracellular active form of TFV, had significantly higher concentrations in duodenum vs rectum, whereas MVC showed the opposite trend, with 5-fold higher rectal concentrations (Table 2).

TPRs represent the extent of drug exposure in tissue relative to plasma. In the duodenum, median TFV TPR was significantly higher than any other drug in this tissue and was significantly higher in duodenum than rectum (median, 717.2 [IQR, 15.3–1102.9] vs 41.2 [IQR, 10.8–99.8]; $P < .001$) (Figure 1A). In the rectum, MVC TPRs were significantly higher than those for FTC, efavirenz, and RAL.

In addition, tissue exposures for all ARVs was greater than the maximum reported 50% inhibitory index (IC_{50}) values from cellular studies, and ranged from 4-fold higher (TFV in rectal tissue) to 1960-fold higher (MVC in rectal tissue) (Figure 1B). Tissue concentrations greater than IC_{50} were present in nearly 100% of subjects, except for 4 samples for FTC and TFV. In the

duodenum, FTC concentrations were above the IC_{50} in 96% of subjects. In the rectum, FTC exposures greater than the IC_{50} were achieved in 92% of subjects, while 88% of subjects had TFV concentrations greater than the IC_{50} (Figure 1B). In sum, ARV concentrations were similar across compartments and largely were at or above the IC_{50}.

We next examined whether ARV tissue concentrations were significantly associated with tissue viral decay by performing linear regression using TPR as the independent variable and HIV RNA and DNA change scores as the dependent variable. No correlations were observed between decreases in HIV DNA or HIV RNA in either duodenal or rectal tissues or when all tissue samples were combined after adjustments were made for biased outliers (Figure 1C and 1D). A similar analysis was performed to assess the effect of TPR on immune reconstitution in GALT as measured by changes in $CD4^+$ T-cells/mm^2 lamina propria or $CD4^+$ T-cell percentage in single-cell suspensions. No significant relationships were observed in either intestinal site for any individual drugs or combinations with any 9-month change in immune cell population (all $P > .05$; data not shown).

DISCUSSION

Our study demonstrates that in tissues where immune reconstitution is most blunted following suppressive cART, ARV drug concentrations exceed the in vitro IC_{50} values. In addition, significant correlations for HIV RNA levels and decay post-cART between peripheral blood and GALT compartments support the hypothesis that these compartments demonstrate an interdependence, as would be expected for this highly vascular tissue. One explanation for how these results differ from previous reports potentially stems from our use of snap-frozen whole tissue for all but the intracellular TFV-dp and emtricitabine triphosphate (FTC-tp) concentrations [4]. Previous reports have used collagenase digestion with multiple wash steps associated with single-cell suspension processing that can be associated with leaching of parent drug concentrations, and can lead to reporting of lower concentrations after processing [4, 11]. However, this is not the case for measuring concentrations of intracellular TFV-dp and FTC-tp, which correlate highly with tissue homogenate concentrations of TFV-dp and FTC-tp [12].

If residual viral replication were driving persistent immune defects in GALT, then some signal with altered TPRs between compartments would have been anticipated. However, we did not find evidence for a significant contribution of residual HIV replication leading to persistent $CD4^+$ T-cell depletion even though TPRs were above the IC_{50} for the multiple classes of ARVs. HIV DNA declined significantly in all 3 compartments and the HIV RNA levels were generally very low or undetectable after treatment. These largely negative data do not exclude a potential contribution to ongoing HIV replication as others have reported in mucosal tissues [7, 13].

The penetration of these ARV medications into these highly vascularized tissues weighs in favor of other local factors (eg, microbial antigen driven inflammation and/or translocation) playing a more dominant role in poor immune reconstitution. However, inhibitory concentrations derived from in vitro cellular studies may not represent the true therapeutic threshold for these agents in tissues, as free drug tissue concentrations can be impacted by protein binding [14]. Additional research is needed in this area. Nonetheless, these novel results emphasize the need to focus on multiple hypotheses to explain heterogeneous immune reconstitution along the gastrointestinal tract. Previous work from our laboratory and others suggests that proinflammatory bacterial antigen initiate profibrotic and other immune activation pathways that interrupt immune reconstitution [15]. Ongoing analysis of these tissue samples seeks to characterize the microbiome within the tissue as potential factor impacting immune reconstitution in these diverse compartments. These investigations may provide additional insights into T-cell kinetics in GALT following effective cART.

Supplementary Data

Supplementary materials are available at *The Journal of Infectious Diseases* online. Consisting of data provided by the authors to benefit the reader, the posted materials are not copyedited and are the sole responsibility of the authors, so questions or comments should be addressed to the corresponding author.

Notes

Acknowledgments. The authors wish to acknowledge the study participants who contributed to this work as well as the University of California, Davis (UCD) Clinical Research Center research (CTSC) staff who made this research possible.

Disclaimer. The results and views do not represent those of Pfizer, which provided funding to UCD for this work.

Financial support. This work was made possible, in part, by the National Center for Research Resources to UCD (grant number UL1-RR024146); University of North Carolina Center for AIDS Research (grant number P30-AI027763); and the Spanish Ministry of Health and Innovation and the Spanish Network on AIDS Research (grant number RD06/006-SSV&TS).

Potential conflicts of interest. All authors: No reported conflicts of interest. All authors have submitted the ICMJE Form for Disclosure of Potential Conflicts of Interest. Conflicts that the editors consider relevant to the content of the manuscript have been disclosed.

References

1. Brenchley JM, Douek DC. HIV infection and the gastrointestinal immune system. Mucosal Immunol **2008**; 1:23–30.
2. Asmuth DM, Ma ZM, Mann S, et al. Gastrointestinal-associated lymphoid tissue immune reconstitution in a randomized clinical trial of raltegravir versus non-nucleoside

reverse transcriptase inhibitor-based regimens. AIDS **2012**; 26:1625–34.
3. Hatano H, Somsouk M, Sinclair E, et al. Comparison of HIV DNA and RNA in gut-associated lymphoid tissue of HIV-infected controllers and noncontrollers. AIDS **2013**; 27:2255–60.
4. Fletcher CV, Staskus K, Wietgrefe SW, et al. Persistent HIV-1 replication is associated with lower antiretroviral drug concentrations in lymphatic tissues. Proc Natl Acad Sci U S A **2014**; 111:2307–12.
5. Lorenzo-Redondo R, Fryer HR, Bedford T, et al. Persistent HIV-1 replication maintains the tissue reservoir during therapy. Nature **2016**; 530:51–6.
6. Serrano-Villar S, Sainz T, Ma ZM, et al. Effects of combined CCR5/integrase inhibitors-based regimen on mucosal immunity in HIV-infected patients naïve to antiretroviral therapy: a pilot randomized trial. PLoS Pathog **2016**; 12:e1005381.
7. Chun TW, Nickle DC, Justement JS, et al. Persistence of HIV in gut-associated lymphoid tissue despite long-term antiretroviral therapy. J Infect Dis **2008**; 197: 714–20.
8. Brown KC, Patterson KB, Malone SA, et al. Single and multiple dose pharmacokinetics of maraviroc in saliva, semen, and rectal tissue of healthy HIV-negative men. J Infect Dis **2011**; 203:1484–90.
9. Patterson KB, Prince HA, Stevens T, et al. Differential penetration of raltegravir throughout gastrointestinal tissue: implications for eradication and cure. AIDS **2013**; 27:1413–9.
10. Thompson CG, Bokhart MT, Sykes C, et al. Mass spectrometry imaging reveals heterogeneous efavirenz distribution within putative HIV reservoirs. Antimicrob Agents Chemother **2015**; 59:2944–8.
11. Cory TJ, Winchester LC, Robbins BL, Fletcher CV. A rapid spin through oil results in higher cell-associated concentrations of antiretrovirals compared with conventional cell washing. Bioanalysis **2015**; 7:1447–55.
12. Yang KH, Hendrix C, Bumpus N, et al. A multi-compartment single and multiple dose pharmacokinetic comparison of rectally applied tenofovir 1% gel and oral tenofovir disoproxil fumarate. PLoS One **2014**; 9:e106196.
13. Yukl SA, Gianella S, Sinclair E, et al. Differences in HIV burden and immune activation within the gut of HIV-positive patients receiving suppressive antiretroviral therapy. J Infect Dis **2010**; 202:1553–61.
14. Cottrell ML, Srinivas N, Kashuba AD. Pharmacokinetics of antiretrovirals in mucosal tissue. Expert Opin Drug Metab Toxicol **2015**; 11:893–905.
15. Asmuth DM, Pinchuk IV, Wu J, et al. Role of intestinal myofibroblasts in HIV-associated intestinal collagen deposition and immune reconstitution following combination antiretroviral therapy. AIDS **2015**; 29:877–88.